Reaction of Rb(5^2D, 7^2S) with H_2

Li-Hsyan Fan, Jye-Jong Chen, Yann-Yow Lin, and Wei-Tzou Luh*

Department of Chemistry, National Chung Hsing University, 250 Kuo-Kuang Road, Taichung 402, Taiwan, Republic of China

Received: November 6, 1998; In Final Form: January 3, 1999

The nascent quantum state distributions of the RbH product resulting from the reaction of Rb($5^2D_{3/2,5/2}$, $7^2S_{1/2}$) with H_2 are determined using a laser pump−probe technique. For the three investigated reactions, the nascent RbH product molecules are found to populate the lowest three vibrational (v = 0, 1, and 2) levels of the ground electronic state. The relative vibrational populations are determined to be (0.42, 0.31, 0.27) for the Rb($5^2D_{3/2}$) + H_2 reaction, (0.42, 0.33, 0.25) for the Rb($5^2D_{5/2}$) + H_2 reaction, and (0.45, 0.32, 0.23) for the Rb($7^2S_{1/2}$) + H_2 reaction, each corresponding to a high vibrational temperature. The nascent RbH rotational temperatures are found to be slightly below the cell temperature. By comparing the spectral intensities of the RbH action spectra with those of pertinent Rb atomic fluorescence excitation spectra, the relative reactivity with H_2 for the three studied atoms is in an order of Rb($7^2S_{1/2}$) > Rb($5^2D_{3/2}$) > Rb($5^2D_{5/2}$). The relative fractions ($\langle f_v\rangle$, $\langle f_R\rangle$, $\langle f_T\rangle$) of average energy disposal are derived as (0.17, 0.04, 0.79) for the Rb($5^2D_{3/2}$) case, (0.17, 0.04, 0.79) for the Rb($5^2D_{5/2}$) case, and (0.14, 0.03, 0.83) for the Rb($7^2S_{1/2}$) case, all having a major translational energy release and a minor rotational energy release. All of the above results support the assumption that the Rb*−H_2 reaction occurs primarily in a collinear $C_{\infty v}$ collision geometry by a harpoon mechanism, in which the crossing between the ionic $Rb^+H_2^-$ energy surface and the neutral Rb*−H_2 energy surfaces plays a very crucial role. A further comparison with two previous results reveals that the average vibrational disposal $\langle f_V\rangle$ in MH changes dramatically as the excited alkali atom M* is varied from K* to Rb* and to Cs*. The $\langle f_V\rangle$ value for the (K* + H_2) system is close to the prior distribution limit, but it becomes smaller and smaller for the (Rb* + H_2) system and for the (Cs* + H_2) system.

I. Introduction

The study of either inelastic or reactive collisions between electronically excited metal atoms and molecules has long been a subject of molecular dynamics.[1−6] For brevity, we focus here only on collisions between electronically excited alkali metal atoms (M*) and diatomic molecules (AB), especially the hydrogen molecule. For inelastic collisions, the electronic-to-vibrational (E−V) energy transfer of the first electronically excited sodium atom has been quite intensively investigated both experimentally[7−11] and theoretically.[12−17] The experiments have been successfully conducted either by a molecular beam method in which the relative translation energies of the receding particles are measured[2,8] or by a laser method in which the internal state distributions of AB(v',J') are measured.[7,10,11] The experimental results reveal that the energy transfer processes are nonresonant and the internal state distributions are nonthermal. They are largely interpreted by a curve-crossing mechanism via either an ionic intermediate model[13−14,17] or a bond-stretch attraction mode.[13] For collisions between H_2 molecules and other alkali metal atoms also in their first $n^2P_{1/2}$ and $n^2P_{3/2}$ fine-structure states, most efforts are focused on measurements of the quenching rate (cross section) of each fine-structure state and the mixing rate between them.[3]

For collisions between high-lying electronically excited alkali atoms and H_2 molecules, reactive processes may become energetically feasible and competitive with inelastic collisions, as demonstrated chronologically in previous studies on Cs*−H_2,[6,18−21] K*−H_2,[22] and Na*−H_2,[23−25] systems. For the Cs*−H_2 system, the reaction between Cs(7^2P) and H_2 was first observed in 1975 as a form of laser snow by Tam et al.,[18] who indirectly excited the Cs atom to its 7^2P state via a far-wing excitation.[4,26] This system was then further investigated by several French groups via a resonant excitation in a series of substantial experimental and theoretical studies.[6,19−20] In a crossed-beam experiment, Crepin et al.[19b] observed that (a) the CsH product was formed in a single collision and (b) the excited Cs atom in the $7^2P_{1/2}$ fine-structure state was more reactive than that in the $7^2P_{3/2}$ fine-structure state, and they attributed the results to a harpooning mechanism along a collinear $C_{\infty v}$ collision geometry:

$$Cs(7P) + H_2 \rightarrow (Cs^+H_2^-) \rightarrow CsH + H$$

This argument was further demonstrated theoretically by Gadea et al.[19c] in a study with diabatic potential energy surfaces and experimentally by L'Hermite et al.[19g] through measurements of angular scattering probabilities and rotationally resolved total cross sections, in which at a collision energy of 0.09 eV the ratio between the reactive cross sections for the two 7P fine-structure states was found to be $\sigma(Cs(7P_{1/2}) + H_2)/\sigma(Cs(7P_{3/2}) + H_2) = 4.2$. In a gas cell experiment, Visticot et al.[20b] found that during the reaction with H_2, the Cs atom in the $6^2D_{3/2}$ fine-structure state had a higher efficiency in producing CsH than that in the $7^2P_{3/2}$ fine-structure state. In the recent study on the reaction of Cs(8^2P) and Cs(9^2P) with H_2, Huang et al.[21] found that (a) the reactivity of the Cs atom at the J = 1/2 fine-structure state was not different from that at the 3/2 fine-structure state,

* To whom correspondence should be addressed. Fax: 886-4-286-2547. E-mail: wtluh@dragon.nchu.edu.tw.

10.1021/jp984334a CCC: $18.00
Published on Web 02/20/1999

(b) the CsH product was produced only in the $v = 0$ and 1 vibrational states, (c) the rotational temperatures of the products were approximately the same as the cell temperature, and (d) about 90% of the available energy was released as translation. They argued that (a) the reaction mechanism was primarily collinear abstraction, not an insertion, and (b) the reaction involved electron transfer at a Cs−H distance not far from the equilibrium bond length, not a harpoon reaction in the usual sense.[19g,27] In a very recent two-step excitation beam study, Vetter[28] and co-workers observed that the Cs(6^{2}D) atom reacted with H_2 to produce CsH but the Cs(8^{2}S) atom did not.

For the K*−H_2 system, the reaction of K* with H_2 was first investigated by Lin and Chang.[22a] They observed that the nascent KH product did result from the reaction of the K atom in its 7^{2}S state but not in its 5^{2}D state. They attributed these state-selective results to the harpoon mechanism in a collinear $C_{\infty v}$ collision geometry. Quite recently, Liu and Lin[22c] measured the rotational quantum state distribution of the nascent KH product from the reaction of K(5^{2}P, 6^{2}P, 7^{2}P) with H_2. Their results, (a) thermal rotational state distribution, (b) high vibrational temperature, and (c) increasing vibrational energy disposal in the order 5P < 6P < 7P, demonstrated that the reaction followed a harpoon mechanism along a collinear collision geometry. Very recently, to resolve the effects of electronic orbital symmetry on chemical reactivity, Liu and Lin[22d] have systematically investigated the reaction of K(n^2S, m^2P, and l^2D) with H_2. In addition to the above three points, they also found that the reactivity followed the order of D < P < S, indicating that the key parameter was the electronic orbital symmetry, not the potential energy. The electronic orbital symmetry would control the possibility of a conical crossing between a neutral K*−H_2 Σ^+ energy surface and the ionic $K^+-H_2^-$ Σ^+ energy surface. In a very recent half-collision study (see the Na*−H_2 system below), Kleiber[23e] and co-workers also found that for the K(5^{2}P)−H_2 system, the predominant reactive process is along the repulsive $^2\Sigma^+$ surface in a collinear collision geometry.

For the Na*−H_2 system, the reaction dynamics of Na(4^{2}P) with H_2 was recently investigated by Kleiber et al.[5,23] In a half-collision study with an elegant far-wing excitation technique, Bililign and Kleiber[23a] have resolved the effects of orbital alignment as well as the reaction characteristics along the attractive surfaces and along the repulsive surfaces, respectively. They found that the nascent NaH products resulting along the attractive surfaces[29] (via a far red-wing excitation) populated preferentially at high rotational states, but those resulting along the repulsive surface[29] (via a far blue-wing excitation) populated preferentially at low rotational states, as what was observed in the Hg(6^{3}P)−H_2 case.[30] In a full-collision study[23b] on the reaction of Na(4^{2}P) with H_2, D_2, and HD, they observed a bimodal rotational distribution but did not reveal any kinematic isotopic effect. They argued that (a) the results were due to the predominant processes along the attractive $^2B_2$ potential energy surface in a near side-on attack C_{2v} geometry and (b) the rotational distribution was determined late in the exit channel.[31] They also suggested that the reaction along the repulsive surface should have a kinematic isotopic effect, which was subsequently demonstrated by their half-collision study.[23c] Using a CARS probing technique, Pichler et al.[25a] observed the NaH product in a Na + H_2 mixture when the Na atom was excited to one of its 3^{2}P, 4^{2}D, and 5^{2}S states. The NaH product of the Na(3^{2}P) + H_2 reaction was attributed to the ensuing reaction of Na(3^{2}P) with vibrationally excited hydrogen molecules, which were produced by an earlier E−V energy transfer between Na(3^{2}P) and H_2.[8−10,32] This argument was lately demonstrated by Motzkus et al.[25b,c] via a comparison between the Na(4p) + H_2 and Na(3p) + H_2 systems and a rate equation model.

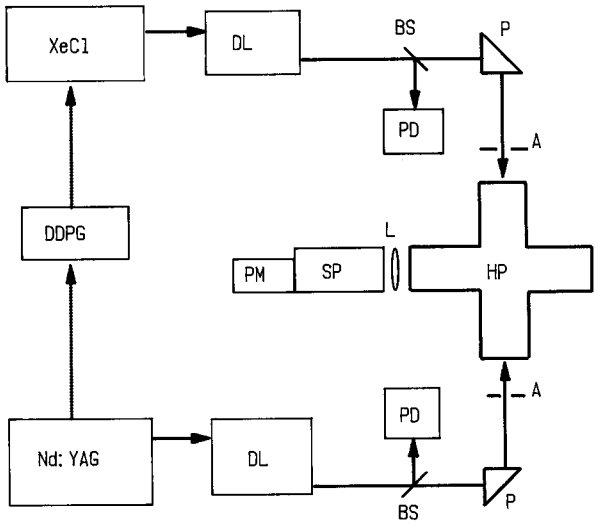

Figure 1. Experimental setup: A, an aperture; BS, a beam splitter; DDPG, a digital delay/pulse generator; DL, a dye laser; HP, the rubidium heat-pipe oven; L, a lens; P, a 90° prism; PD, a photodiode; PM, a photomultiplier; SP, a monochromator.

For the Rb*−H_2 system, only a few experimental works have been published.[3] In 1970, Hrycyshyn and Krause[33] reported cross sections for the fine-structure mixing and quenching of Rb(5^{2}P$_J$) due to collisions with H_2. In 1983, Cuvellier et al.[34] reported that a pronounced influence of rotational energy on the fine-structure mixing cross section of Rb(5^{2}P$_J$) was found for two particular rotational levels of D_2 but none in the case of H_2. Later, they[35] also found a near-resonant electronic-to-rotational energy transfer process during the collision study between Rb(7S) atoms and H_2 molecules. Recently, we planned a long-term research effort to study inelastic and reactive collisional processes in the Rb*−H_2 system. In a recent article,[32] we reported the E−V energy transfer between Rb(5^{2}P$_J$) and H_2. For an electronically excited rubidium Rb(n^2L) atom lying above its 6^{2}S$_{1/2}$ state, reactive processes become energetically feasible.

In this article, we report the nascent quantum state distributions of the RbH product of the reaction of Rb(5^{2}D and 7^{2}S) with H_2. We use a laser pump−probe technique to detect the nascent RbH product. Section II describes the experimental details. Section III presents the results and discussions. The conclusion is presented in section IV.

II. Experiment

Our experimental setup is sketched in Figure 1, in which the parts for signal processing are not shown. A frequency-doubled 10 Hz Q-switched Nd:YAG laser (Lumonics YM600), having a pulse width of 7 ns and operating at a typical pulse energy of 30 mJ, was used to pump a dye laser (Lumonics HD500) in order to generate a 6 ns PUMP laser beam for preparing electronically excited Rb(5^{2}D) and Rb(7^{2}S) atoms. The active medium was a methanol solution of a laser dye LDS759 (Exciton), covering an active spectral range of 730−790 nm. A XeCl excimer laser (Lambda Physik LPX100), having a pulse width of 20 ns and operating at a typical pulse energy of 60 mJ, was used to pump another dye laser (Lambda Physik FL3002) in order to generate a probe laser beam for detecting the nascent RbH product. A methanol solution of a laser dye Coumarin 503 (Exciton) was used as an active medium to cover the pertinent 500−530 nm spectral range of the RbH $A^1\Sigma^+$−$X^1\Sigma^+$ electronic transition. For the pump laser, the laser pulse

energy was varied between 0.1 and 1 mJ. However, a true two-photon excitation could only be assured when the pulse energy was kept below 0.2 mJ. The results at a laser pulse energy 0.15 mJ will be presented below. For the probe laser, the laser pulse energy was kept at 0.3 mJ in order to saturate a RbH A−X excitation and to simplify the retrieval of the nascent quantum state distributions (see section III.C below). The line widths were 0.04 cm^{-1} for the pump laser and 0.2 cm^{-1} for the probe laser. A Ne calibration lamp (Oriel) was used to calibrate the laser wavelength. The uncertainty of wavelength measurements was about 0.01 nm. The pump laser beam was directed along the axis of the longer arms of a five-arm crossed heat-pipe oven, but the probe laser beam was oppositely directed in a small crossing angle to overlap only the observing region. The pulse delay (τ_D) between the probe laser pulse and the pump laser pulse was governed by a digital delay/pulse generator (SRS DG535). The reaction cell was a heat-pipe oven, and 25 g of naturally abundant rubidium metal (STREM, 3 N+) were loaded in its center. The cell was typically operated at a temperature of 453 K, at which the rubidium vapor pressure[36] was about 20 mTorr and the RbH A−X rovibrational transition line had a Doppler width of about 0.03 cm^{-1}. About 5 Torr of H_2 gas was filled in the cell for use both as a buffer gas and as a reaction partner. The induced A−X fluorescence was observed along a perpendicular arm by an interference-detection system, which was composed of a monochromator (ARC SP275) and a photomultiplier tube (Hamamatsu R928 or R943-02). The detector signal was fed into a boxcar averager−gated integrator system (SRS SR250); the averaged output was then recorded by a personal computer for later data treatment.

In this work, three types of spectra were measured. The first spectrum was a fluorescence excitation (FE) spectrum in which the pump laser was first tuned to a particular two-photon atomic transition and the induced RbH A−X fluorescence at a particular vibrational (v',v'') transition band was then monitored by scanning the probe laser across the pertinent vibrational (v',v) transition band in order to determine the nascent rotational quantum state distribution of the vibrational level v. Both the (v',v'') fluorescence band and the (v',v) excitation band were selected to have a favorable Franck−Condon factor, which could be calculated by an INTENSITY program[37] with the given potential curves[38] for the A and X electronic states of ^{85}RbH. Note that we took the isotopic ^{85}RbH molecule as the reaction product, although about 28% of the RbH product molecules were expected to be of ^{87}RbH, whose spectral transition lines could not be resolved with the probe laser line width mentioned above. The second spectrum was an action spectrum[29a] in which the probe laser was tuned to a particular A−X rovibrational transition and then the pump laser was scanned across the spectral range covering the rubidium 5^2S-5^2D and 5^2S-7^2S two-photon atomic transitions. The action spectrum detected those excited Rb atoms lying near the $5^2D_{5/2,3/2}$ fine-structure states and the $7^2S_{1/2}$ state, which would react to produce RbH. The fluorescence excitation spectrum and the action spectrum could be taken at various pulse delays. The third spectrum was a time-resolved spectrum in which the pump laser was tuned to a particular two-photon atomic transition and the probe laser was tuned to a particular RbH A−X rovibrational transition; the detector signals at various pulse delays were then recorded by a digital oscilloscope (LeCroy 9360).

III. Results and Discussions

A. RbH Fluorescence Excitation Spectra. From observed fluorescence excitation spectra, we find that the nascent RbH product molecules, resulting from the reaction between H_2 molecules and electronically excited Rb($5^2D_{3/2}$, $5^2D_{5/2}$, or $7^2S_{1/2}$) atoms, populated only at the lowest three vibrational ($v = 0$, 1, and 2) levels of the ground electronic state. Our selected fluorescence-excitation (v',v'')−(v',v) band combinations are separately (8,1)−(8,0) for the $v = 0$ level, (9,0)−(9,1) for the $v = 1$ level, and (13,0)−(13,2) for the $v = 2$ level. Two observed FE spectra of the RbH ($v = 2$) product, resulting separately from the Rb($5^2D_{5/2}$) atom and the $7^2S_{1/2}$ atom, are shown in Figure 2, in which pertinent spectral assignments are identified by using the given Dunham-type coefficients[38] for the A and X electronic states of RbH. With our typical experimental conditions, the pressure of H_2 at 4.6 Torr, the oven temperature at 453 K, and the pulse delay τ_D at 15 ns, the probability that the nascent RbH product would experience a secondary collision was only about 0.32, assuming a collision cross section[21,22a] of 10 Å^2 between RbH molecules and H_2 molecules. Our observed FE spectra may thus be attributed to the nascent RbH product.

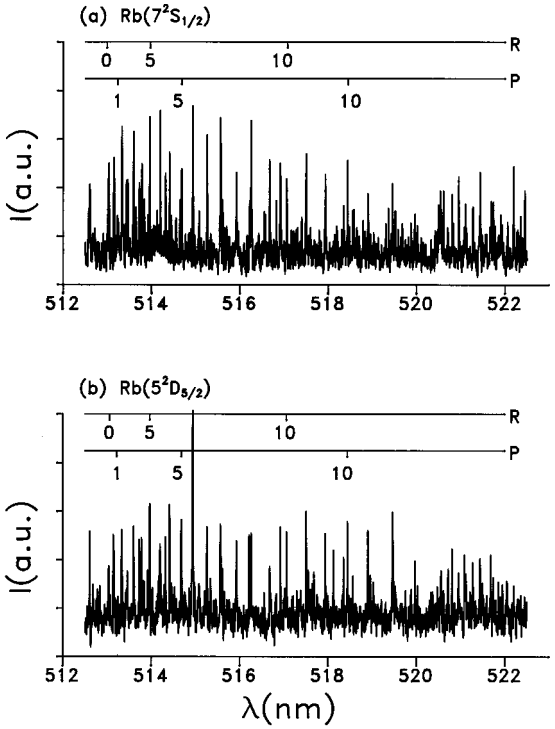

Figure 2. Fluorescence excitation spectra of the nascent RbH ($v = 2$) product: (a) the reaction Rb($7^2S_{1/2}$) + H_2; (b) the reaction Rb($5^2D_{5/2}$) + H_2 [$T = 453$ K, $P(H_2) = 4.6$ Torr, and $\tau_D = 15$ ns].

B. Reactivity of Electronically Excited Rb* Atoms. Our RbH FE spectra revealed that for the RbH yield, the reaction of Rb(5^2D) + H_2 was more efficient than the Rb($7^2S_{1/2}$) + H_2 reaction. For other M*−H_2 cases, Pichler et al.[25] observed that for the NaH yield, the reaction Na(4^2D) + H_2 was as efficient as the reaction Na(5^2S) + H_2 (see Figure 5, of ref 25); Lin and co-workers[22a,d] observed that the nascent KH yield was high for the reaction of the K(7^2S) atom but very low for the K(5^2D) atom; Vetter[28] and co-workers found very recently that the Cs(6^2D) atom reacted with H_2 to produce CsH, but the excited Cs(8^2S) atom did not. Thus, there were some discrepancies among the above four different alkali−hydrogen systems.

To further confirm our observations, both action spectra at several laser pulse delays and time-resolved spectra have been measured at a particular pump laser pulse energy. Two action spectra for the RbH ($v = 2$, $J = 5$) product at a 10 ns laser pulse delay are reproduced in Figure 3, from which one can find that (a) the Rb($5^2D_{3/2,5/2}$) atom is at least as efficient as the

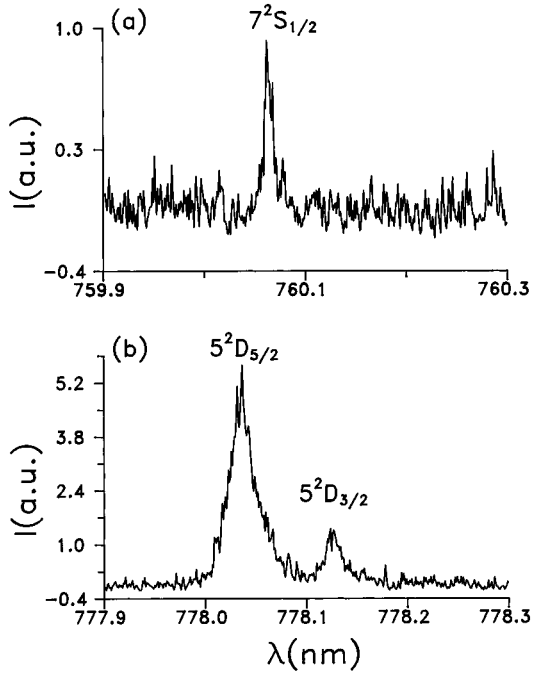

Figure 3. Action spectra for the RbH product at its X(2,5) rovibrational level resulting from electronically excited Rb atoms near (a) the $7^2S_{1/2}$ state and (b) the $5^2D_{5/2}$ state [T = 453 K, $P(H_2)$ = 5.6 Torr, and τ_D = 10 ns].

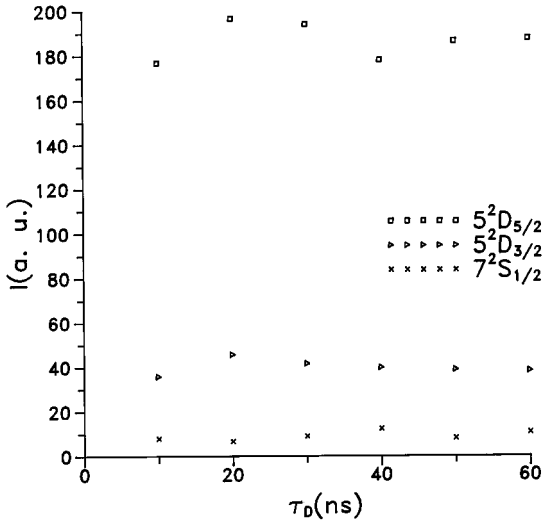

Figure 4. Plot of integrated action spectral intensities with respect to the laser pulse delays τ_D [T = 453 K and $P(H_2)$ = 5.6 Torr].

$Rb(7^2S_{1/2})$ atom in producing the RbH product and (b) the spectral line widths (fwhm) for the $5^2D_{3/2}$ and $5^2D_{5/2}$ substates are of ~0.33 cm^{-1}, that of ~0.17 cm^{-1} for the $7^2S_{1/2}$ state. Several action spectra have been also taken at various laser pulse delays $\tau_D \leq 60$ ns; they have been integrated over the active spectral range, and the results reveal that total action intensities for the $5^2D_{3/2}$ and $5^2D_{5/2}$ fine-structure states are consistently higher than that for the $7^2S_{1/2}$ state, as shown in Figure 4; their averaged relative ratios are 4.4($5^2D_{3/2}$), 20.6($5^2D_{5/2}$), and 1.0($7^2S_{1/2}$). Such a result indicates that the reacted amount of electronically excited Rb* atoms lying at and near their $5^2D_{3/2}$ or $5^2D_{5/2}$ fine-structure states is higher than that of electronically excited Rb* atoms lying at and near their $7^2S_{1/2}$ state.

In fact, the actual RbH yield varies with both (a) the reactivity of a particular electronically excited Rb* atom and (b) its number density, which in turn depends on the rate of two-photon excitation. Thus, if the relevant two-photon transition rates are given, we may derive the relative reactivities for the three different electronically excited Rb($5^2D_{3/2}$, $5^2D_{5/2}$, or $7^2S_{1/2}$) atoms from the observed spectral intensities. We are unable to do this since only the $5^2S_{1/2}-5^2D_{3/2}$ and $5^2S_{1/2}-5^2D_{5/2}$ two-photon transition rates are available from the literature.[39] However, we may still roughly estimate the relative reactivities of the three electronically excited Rb* atoms by comparing some nascent RbH action spectral intensities with their relevant atomic fluorescence excitation spectral intensities, which are proportional to the Einstein A coefficients as well as the number density of excited Rb* atoms. Note that in order to mimic most measurements performed for detecting the nascent RbH product, we integrate and compare only the 0.04 cm^{-1} spectral range around the line center of each spectral peak.

Three relevant atomic transitions are $7^2S_{1/2}-5^2P_{3/2}$, $5^2D_{5/2}-5^2P_{3/2}$, and $5^2D_{3/2}-5^2P_{1/2}$, and their respective Einstein A coefficients are 4.40 × 10^6, 2.70 × 10^6, and 2.44 × 10^6 s^{-1}, which were derived from the known oscillator strengths (f),[40] 0.0181, 0.0366, and 0.0425, by using the relation[41] $A = [g_1/(1.499\lambda^2 g_2)]f$. The fluorescence excitation spectra for the above three atomic transitions are measured at a pump laser pulse energy of 0.15 mJ. By taking into account the above Einstein A coefficients and by scaling the laser pulse energy to the same photon flux density, the relative number densities of the excited Rb* atoms at the $7^2S_{1/2}$, $5^2D_{5/2}$, and $5^2D_{3/2}$ states are found to be in a ratio of 100:1740(57):297(69). The action spectra are taken at the RbH A−X(13,2)R(5) line; the relative RbH yields due to the excited Rb* atoms at $7^2S_{1/2}$, $5^2D_{5/2}$ and $5^2D_{3/2}$ states are measured to be in a ratio of 100:354(70):114(25). By combining the above data, we obtain a relative reactivity ratio of 100:20(12):38(17). Thus, the relative reactivity with H_2 for the three studied atoms is in an order of Rb($7^2S_{1/2}$) > Rb($5^2D_{3/2}$) > Rb($5^2D_{5/2}$). Note that the above quantities are each an average from three different measurements, and the numbers in parentheses represent one standard deviation for the last two digits. The derived relative reactivity reflects that among the three studied electronically excited Rb* atoms, the Rb($7^2S_{1/2}$) atom is the most reactive atom, then the Rb($5^2D_{3/2}$) atom, and the Rb($5^2D_{5/2}$) atom is the least reactive one.

Our derived relative reactivity is in general consistent with the previous conclusion made by Lin and co-workers,[22a,d] who attributed the low reactivity of the excited K(^{2}D) atom to its unfavorable electronic orbital symmetry, provided that the reaction followed a harpoon mechanism along a collinear collision $C_{\infty v}$ geometry. Under such a reaction mechanism, every M(n^2S) atom may enter the reactive M*−H_2 Σ^+ energy surface, however, only one-fifth of M(n^{2}D) atoms and one-third of M(n^2P) atoms may statistically have such a possibility.

TABLE 1: Nascent Quantum State Distributions for the Three Rb* + H_2 Reactions[a]

Rb*	P_0	P_1	P_2	T_R	T_v	$\langle E_V \rangle$
Rb($5^2D_{3/2}$)	0.42(4)	0.31(2)	0.27(2)	405(77)	5755(907)	765
Rb($5^2D_{5/2}$)	0.42(1)	0.33(1)	0.25(1)	388(57)	4861(62)	743
Rb($7^2S_{1/2}$)	0.45(1)	0.32(1)	0.23(1)	373(44)	3827(6)	702

[a] P_0, P_1, and P_2 represent separately the relative populations for the nascent vibrational levels v = 0, 1 and 2; T_R and T_v are respectively an averaged rotational temperature and a statistical vibrational temperature (both in K); $\langle E_V \rangle$ is an averaged vibrational energy disposal (in cm^{-1}).The numbers in parentheses represent one standard deviation.

C. Nascent Quantum State Distributions. The RbH fluorescence excitation intensities are used to retrieve the rotational and vibrational quantum sate distributions of the nascent RbH product. For a saturated excitation scheme, only the Franck−

TABLE 2: Disposal of Available Energy E_{Avl} in Reactions of Excited Alkali Atoms M(n^2L) with H_2[d]

M(n^2L)	E_{avl}	IP	$\langle f_V\rangle$[a]	$\langle f_R\rangle$[a]	$\langle f_T\rangle$[a]	v_{open}	v_{obs}	ref
K(5^2P)	10.84	1.277	0.27	0.09	0.64	4	3	22c
K(6^2P)	23.73	0.744	0.24	0.04	0.72	10	3	22c
K(7^2P)	29.59	0.488	0.28	0.03	0.69	13	3	22c
K(6^2S)	19.08	0.937	0.28	0.05	0.67	7	3	22d
K(7^2S)	27.21	0.587	0.25	0.03	0.72	11	3	22d
Rb($5^2D_{3/2}$)	12.82	0.990	0.17	0.04	0.79	5	2	this work
Rb($5^2D_{5/2}$)	12.83	0.989	0.17	0.04	0.79	5	2	this work
Rb($7^2S_{1/2}$)	14.57	0.914	0.14	0.03	0.83	6	2	this work
Cs($8^2P_{1/2}$)	13.46[b]	0.706	0.05	0.06	0.89	5	1	21
Cs($8^2P_{3/2}$)	13.69[b]	0.696	0.05	0.06	0.89	5	1	21
Cs($9^2P_{1/2}$)	18.97[b]	0.467	0.035	0.035	0.93	8	1	21
Cs($9^2P_{3/2}$)	19.10[b]	0.462	0.035	0.035	0.93	8	1	21
			0.2857[c]	0.2857[c]	0.4286[c]			

[a] $\langle f_V\rangle = \langle E_V\rangle/E_{avl}$; $\langle f_R\rangle = \langle E_R\rangle/E_{avl}$; $\langle f_T\rangle = 1 - \langle f_V\rangle - \langle f_R\rangle$. [b] Modified from the terms E_{avl} listed in Table 2 of ref 21 by adding the available thermal energy 2.5*RT*. [c] The prior distribution limits are of $\langle f_V\rangle = 2/7$, $\langle f_R\rangle = 2/7$, and $\langle f_T\rangle = 3/7$. [d] E_{avl} (kcal/mol) = $E^* + D_o(MH) - D_o(H_2) + 2.5RT$. E^* and D_o represent the excited energy of the M(n^2L) state and the dissociation energy of a diatomic molecule, respectively; IP is the ionization potential (eV) of each state; $\langle f_V\rangle$, $\langle f_R\rangle$, and $\langle f_T\rangle$ represent separately the relative fraction of average energy disposal among vibration, rotation and translation; v_{open} and v_{obs} are respectively the highest open and observed vibrational level of the product MH.

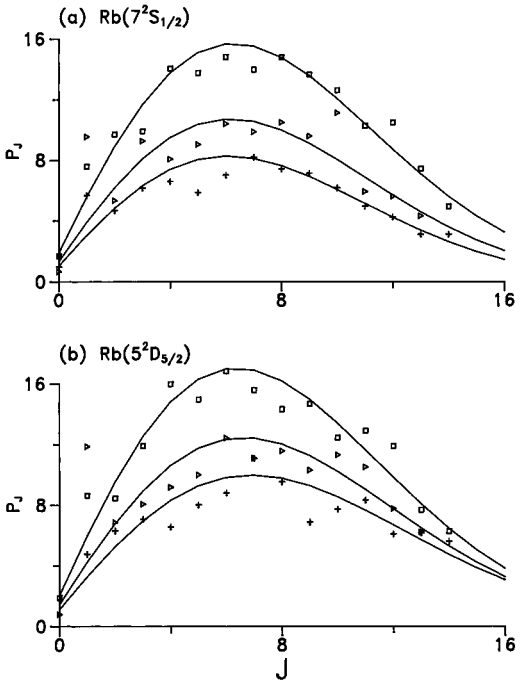

Figure 5. Rotational quantum state distributions P_J for the RbH product of (a) the reaction Rb($7^2S_{1/2}$) + H_2 and (b) the reaction Rb($5^2D_{5/2}$) + H_2. Squares represent the derived distributions for the $v = 0$ vibrational level, triangles those for the $v = 1$ level, and crosses those for the $v = 2$ level. Each solid line represents a best least-squares thermal fit.

Condon factors for selected fluorescence bands (v',v'') have to be taken into account. The rotational quantum state distributions P_J for the three observed vibrational levels are derived and averaged over four different measurements, and only the parts for the $5^2D_{5/2}$ case and those for the $7^2S_{1/2}$ case are reproduced in Figure 5. The resultant relative vibrational populations, P_v, averaged rotational temperatures, vibrational temperatures, and averaged vibrational disposals for the nascent RbH product are summarized in Table 1. The nascent RbH molecules are found to populate (1) at low rotational temperatures, slightly below the cell temperature, and (2) at rather high vibrational temperatures. These two points reveal that the reaction occurs primarily via a collinear collision geometry.

With the above quantum state distributions, one may determine average energy disposals among the three modes: vibration of RbH, rotation of RbH, and relative translation of the recoiling RbH + H. The resultant fractions $\langle f\rangle$ are summarized in Table 2, in which previous results for the Cs*−H_2 case[21] and the K*−H_2 case[22c,d] are also included for comparison. Note that the results of Huang et al.[21] are slightly modified to take into account the available thermal energy, 2.5*RT*. From Table 2, one may tell (1) that for each studied (M* + H_2) system, (a) the average energy disposal is in the order $\langle f_R\rangle < \langle f_V\rangle < \langle f_T\rangle$, (b) a major amount of available energy is released into translation; (c) the average rotational disposal $\langle f_R\rangle$ in MH is far from the prior distribution, and (d) except for the (K(5^2P) + H_2) system, the highest observed vibrational level v_{obs} for each listed (M* + H_2) system is well below the highest open vibrational level v_{open} in energy, and (2) that for the three (M* + H_2) systems, the average vibrational disposal $\langle f_V\rangle$ in MH changes dramatically as the excited alkali atom M* is varied from K* to Rb* and to Cs*. The $\langle f_V\rangle$ value for the (K* + H_2) system is close to the prior distribution limit, but it becomes smaller and smaller for the (Rb* + H_2) system and for the (Cs* + H_2) system.

IV. Conclusion

Three reactions, Rb($5^2D_{3/2}$) + H_2, Rb($5^2D_{5/2}$) + H_2, and Rb($7^2S_{1/2}$) + H_2, have been studied for the first time by a laser pump−probe technique. The nascent RbH molecules for each reaction are found to populate only the lowest three vibrational ($v = 0$, 1, and 2) levels of the ground electronic state. The relative vibrational populations correspond to distributions at a high temperature. The nascent rotational distribution in each vibrational level is at a temperature slightly below the cell temperature. The relative reactivity with H_2 for the three studied atoms is in an order of Rb($7^2S_{1/2}$) > Rb($5^2D_{3/2}$) > Rb($5^2D_{5/2}$). All the above results support the assumption that the Rb*−H_2 reaction occurs primarily in a collinear $C_{\infty v}$ collision geometry by a harpoon mechanism in which the crossing between the ionic $Rb^+H_2^-$ energy surface and the neutral Rb*−H_2 energy surfaces plays a very crucial role. Energy disposals among three modes are derived, and the results are compared with the previous results for the K* + H_2 reaction and the Cs* + H_2 reaction. A further comprehensive study is definitely desirable for resolving the discrepancies among different alkali−hydrogen reaction systems.

Acknowledgment. This work is partly supported by the National Science Council of the Republic of China under Contracts NSC86-2113-M-005-019-L2 and NSC87-2113-M-005-010. We thank Profs. P. D. Kleiber, K. C. Lin, and R. Vetter

for helpful discussions and the referees for valuable comments and suggestions.

References and Notes

(1) Lemont, S.; Flynn, G. W. *Annu. Rev. Phys. Chem.* **1977**, *28*, 261.
(2) Hertel, I. V. *Adv. Chem. Phys.* **1981**, *45*, 341. Hertel, I. V. In *Dynamics of the Excited State*; Lawley, K. P., Ed.; Wiley: New York, 1982; p 475 and references therein.
(3) Breckenridge, W. H.; Umemoto, K. In *Dynamics of the Excited State*; Lawley, K. P., Ed.; Wiley: New York, 1982; p 326.
(4) Mestdagh, J. M.; Baldo, B. A.; Covinsky, M. H.; Weiss, P. S.; Vernon; Schmidt, H.; Lee, Y. T. *Faraday Discuss. Chem. Soc.* **1987**, *84*, 145.
(5) Kleiber, P. D.; Stwalley, W. C.; Sando, K. M. *Annu. Rev. Phys. Chem.* **1993**, *44*, 13.
(6) Gonzalez-Urena, A.; Vetter, R. *J. Chem. Soc., Faraday Trans.* **1995**, *91*, 389; *Int. Rev. Phys. Chem.* **1996**, *15*, 375.
(7) Hsu, D. S. Y.; Lin, M. C. *Chem. Phys. Lett.* **1976**, *42*, 78; *J. Chem. Phys.* **1980**, *73*, 2188.
(8) Hertel, I. V.; Hofmann, H.; Rost, K. A. *Phys. Rev. Lett.* **1976**, *36*, 861; *Chem. Phys. Lett.* **1977**, *47*, 163; *Phys. Rev. Lett.* **1977**, *38*, 343; *J. Chem. Phys.* **1979**, *71*, 674.
(9) Botschwina, P.; Meyer, W.; Hertel, I. V.; Reiland, W. *J. Chem Phys.* **1981**, *75*, 5438.
(10) Hering, P.; Cunha, S. L.; Kompa, K. L. *J. Phys. Chem.* **1987**, *91*, 5459.
(11) Correia, R. R. B.; Pichler, G.; Cunha, S. L.; Hering, P. *Chem. Phys. Lett.* **1990**, *175*, 354.
(12) Magee, J. L.; Ri, T. *J. Chem. Phys.* **1941**, *9*, 638.
(13) Laidler, K. J. *J. Chem. Phys.* **1942**, *10*, 34.
(14) Bjerre, A.; Nikitin, E. E. *Chem. Phys. Lett.* **1967**, *1*, 179.
(15) Levine, R. D.; Bernstein, R. B. *Chem. Phys. Lett.* **1972**, *15*, 1.
(16) Gonzaliez, M. A.; Karl, G.; Watson, P. J. S. *J. Chem. Phys.* **1972**, *57*, 4054.
(17) Andreev, E. A. *Chem. Phys. Lett.* **1973**, *23*, 516.
(18) Tam, A.; Moe, G.; Happer, W. *Phys. Rev. Lett.* **1975**, *35*, 1630.
(19) (a) Picque, J. L.; Verges, J.; Vetter, R. *J. Phys.* **1980**, *41*, L305. (b) Crepin, C.; Picque, J. L.; Rahmat, G.; Verges, J.; Vetter, R.; Gadea, F. X.; Pelissier, M.; Spiegelmann, F.; Malrieu, J. P. *Chem. Phys. Lett.* **1984**, *110*, 395. (c) Gadea, F. X.; Spiegelmann, F.; Pelissier M.; Malrieu, J. P. *J. Chem. Phys.* **1986**, *84*, 4872. (d) Rahmat, G.; Spiegelmann, F.; Verges, J.; Vetter, R. *Chem. Phys. Lett.* **1987**, *135*, 459. (e) Gadea, F. X.; Durup, J. *Chem. Phys. Lett.* **1987**, *138*, 43. (f) Gadea, F. X.; L'Hermite, J.-M.; Rahmat, G.; Vetter, R. *Chem. Phys. Lett.* **1988**, *151*, 183. (g) L'Hermite, J.-M.; Rahmat G.; Vetter, R. *J. Chem. Phys.* **1990**, *93*, 434; **1991**, *95*, 3347. (h) L'Hermite, J.-M. *J. Chem. Phys.* **1992**, *97*, 6215.
(20) (a) Sayer, B.; Ferray, M.; Lozingot L.; Berlande, J. *J. Chem. Phys.* **1981**, *75*, 1894. (b) Visticot, J. P.; Ferray, M.; Lozingot, L.; Sayer, B. *J. Chem. Phys.* **1983**, *79*, 2839.
(21) Huang, X.; Zhao, J.; Xing, G.; Wang, X.; Bersohn, R. *J. Chem. Phys.* **1996**, *104*, 1338.
(22) (a) Lin, K. C.; Chang, H. C. *J. Chem. Phys.* **1989**, *90*, 6151. (b) Luo, Y. L.; Lin, K. C.; Liu, D. K.; Liu, H. J.; Luh, W. T. *Phys. Rev. A* **1992**, *46*, 3834. (c) Liu, D. K.; Lin, K. C. *J. Chem. Phys.* **1996**, *105*, 9121. (d) Liu, D. K.; Lin, K. C. *J. Chem. Phys.* **1997**, *107*, 4244.
(23) (a) Bililign, S.; Kleiber, P. D. *Phys. Rev. A* **1990**, *42*, 6938. (b) *J. Chem. Phys.* **1992**, *96*, 213. (c) Bililign, S.; Kleiber, P. D.; Kearney, W. R.; Sando, K. M. *J. Chem. Phys.* **1992**, *96*, 218. (d) Kleiber, P. D.; Wong, T. H.; Bililign, S. *J. Chem. Phys.* **1993**, *98*, 1101. (e)Kleiber, P. D. Private communication.
(24) Sevin, A.; Chaquin, P. *Chem. Phys.* **1985**, *93*, 49.
(25) (a) Pichler, G.; Motzkus, M.; Cunha, S. L.; Correia, R. R. B.; Kompa, K. L.; Hering, P. *Nuovo Cimento D* **1992**, *14*, 1065. (b) Mtzkus, M.; Pichler, G.; Kompa, K. L.; Hering, P. *J. Chem. Phys.* **1997**, 106, 9057. (c) Mtzkus, M.; Pichler, B.; Kompa, K. L.; Hering, P. *J. Chem. Phys.* **1998**, *108*, 9291.
(26) Herzberg, G. *Spectra of Diatomic Molecules*; Van Nostrand Reinhold: Princeton, New Jersey, 1950; p 397.
(27) Herschbach, D. R. *Adv. Chem. Phys.* **1966**, *10*, 319.
(28) Vetter, R. Private communication.
(29) (a) Breckenridge, W. H.; Jouvet, C.; Soep, B. *J. Chem. Phys.* **1986**, *84*, 1443. (b) Nedelec, O.; Giroud, M. *Chem. Phys. Lett.* **1990**, *165*, 329.
(30) Breckenridge, W. H.; Umemoto, H. *J. Chem. Phys.* **1981**, *75*, 4153; **1984**, *80*, 4168.
(31) Breckenridge, W. H.; Wang, J. H. *Chem. Phys. Lett.* **1987**, *137*, 195.
(32) Chen, M. L.; Lin, W. C.; Luh, W. T. *J. Chem. Phys.* **1997**, *106*, 5972.
(33) Hrycyshyn, E. S.; Krause, L. *Can. J. Phys.* **1970**, *48*, 2761.
(34) Cuvellier, J.; Mestdagh, J. M.; Ferray, M.; de Pujo, P. *J. Chem. Phys.* **1983**, *79*, 2848.
(35) Cuvellier, J.; Petitjean, L.; Mestdagh, J. M.; Paillard, D.; de Pujo, P.; Berlande, J. *J. Chem. Phys.* **1986**, *84*, 1451.
(36) Mozgovoi, A. G.; Novikov, I. I.; Pokrasin, M. A.; Roschupkin, V. V. *High Temp.-High Pressures* **1987**, *19*, 425.
(37) Zemke, W. T.; Stwalley, W. C. *Quantum Chem. Prog. Exch. Bull.* **1984**, *4*, 79.
(38) Kato, H.; Toyosaka, Y.; Suzuki, T. *Bull. Chem. Soc. Jpn.* **1985**, *58*, 562; Stwalley, W. C.; Zemke, W. T.; Yang, S. C. *J. Phys. Chem. Ref. Data* **1991**, *20*, 154.
(39) Marinescu, M.; Florescu, V.; Dalgarno, A. *Phys. Rev. A* **1994**, *49*, 2714.
(40) von der Goltz, D.; Hansen, W.; Richter, J. *Physica Scripta.* **1984**, *30*, 244.
(41) Steinfeld, J. I. *Molecules and Radiation*, 2nd ed; Cambridge: Massachusetts, 1986; p 31.